Turkish Journal of Electrical Engineering & Computer Sciences

http://journals.tubitak.gov.tr/elektrik/

Research Article

Turk J Elec Eng & Comp Sci
(2018) 26: 1027 – 1040

doi:10.3906/elk-1701-112

Design and comparison of embedded air coils for small satellites

Anwar ALI[1,*], **Zeeshan MUKHTAR**[1], **Khalil ULLAH**[1], **Leonardo REYNERI**[2]
[1]Department of Electrical Engineering, National University of Computer & Emerging Sciences, Peshawar Campus, Pakistan
[2]Politecnico di Torino, Turin, Italy

Received: 11.01.2017 • **Accepted/Published Online:** 12.11.2017 • **Final Version:** 30.03.2018

Abstract: The paper discusses the comparison of different shapes of embedded air coils for the attitude control of small satellites. Various systems are available in the market for the attitude control of small satellites such as reaction wheels, permanent magnets, magnetic rods, and thrusters. The available systems have large size, heavier weight, and relatively higher power consumption. A miniaturized system with less power consumption and heat dissipation is required that can provide the anticipated torque. This paper focuses on the design and comparison of square and circular air coils embedded in four internal layers (i.e. 2nd, 3rd, 4th, and 5th) of the eight layer CubeSat power management tile (CubePMT) PCB. Each layer has 50 turns of copper traces and four layers have a total of 200 turns. The four embedded coils are reconfigurable and can be connected in different configurations (single, series, parallel, and hybrid) through switches. The two shapes are compared on the basis of dipole moment, torque generated, power dissipated, time of rotation, and thermal heat generation.

Key words: Attitude control, dipole moment, power dissipation, torque, thermal modeling

1. Introduction

CubeSat, with dimensions 10 × 10 × 10 cm^3 and mass less than 1.33 kg, can be used for earth observation, spying, and different subsystems' testing in the space environment [1,2]. Because of its small size, low weight, low cost, and short development time many universities around the world are working on CubeSat projects. The Department of Electronics and Telecommunication (DET) at Politecnico di Torino has been working on a nano-satellite project called AraMiS since 2002 and developing small satellites and modules of different shapes and size. The main problem with small satellites is the available space and weight constraints for housing a large number of required subsystems such as power, attitude determination and control, telecommunication, and payload. The most applicable solution is the miniaturization of these subsystems to make them lighter and smaller. DET developed a 1U CubeSat dimension satellite called AraMiS-C1 as shown in Figure 1, with all subsystems mounted on two types of tiles called CubeSat power management tile (CubePMT) and CubeSat telecommunication tile (CubeTCT). CubePMT is shown in Figure 2, which contains power management, attitude determination sensors, and attitude actuation systems.

For orientation and stabilization of CubeSat in space, an attitude control system is used, i.e. to bring solar panels in line with the sun and the antenna towards the ground station. For attitude control of the CubeSat different systems are available in the market like permanent magnets, reaction wheel, and magnetic

*Correspondence: anwar.safi@nu.edu.pk

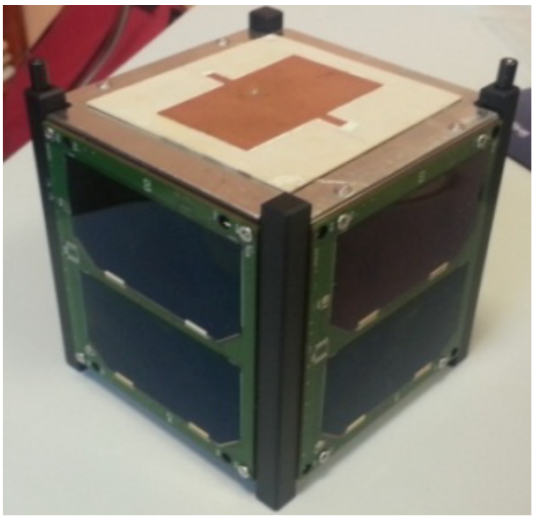

Figure 1. Photograph of AraMiS-C1.

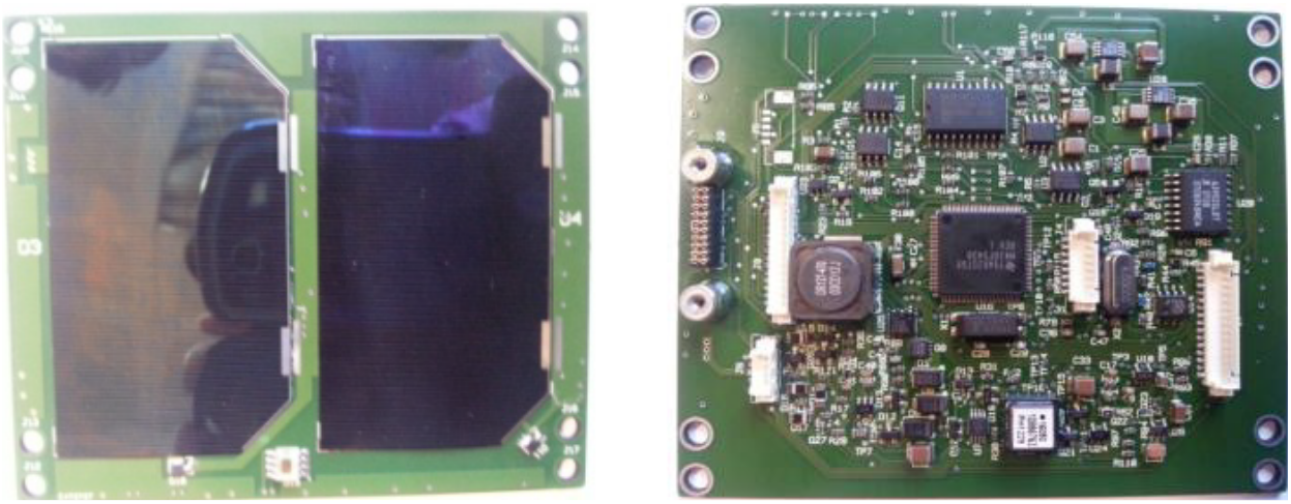

Figure 2. Photograph of solar panel and component side of CubePMT module.

rods [3,4]. Each of them has its own pros and cons. Permanent magnets are cheaper, simple, lightweight, and dissipate no power, but the problem is the inadequate pointing accuracy and they give very little choice in the pointing direction. Pointing accuracy and orientating the satellite in any direction is better done by reaction wheels and magnetic rods but their price, weight, and size make them inappropriate for CubeSat dimension nanosatellites.

For attitude control and stabilization of AraMiS-C1, an air coil was designed and embedded in the CubePMT tile PCB four internal layers. This embedded air coil is a good choice for attitude control [5] because of its small dimensions, lower weight, minimum heat dissipation, and reconfigurability.

For embedded air coils there were many choices regarding shape but the best were the square and circular ones. This paper discusses the design and comparison of the two different shapes, square and circular embedded air coils, on the basis of dipole moment generation, resultant torque, power consumption, and heat generation.

The embedded air coils were analyzed on the basis of these parameters and the best one was selected and implemented in the CubePMT PCB internal layers of AraMiS-C1.

This paper is an extension of previous work [6,7]. It is organized as follows. Following this introduction, the next section explains the working principle of air coils. The proceeding section elaborates on the design of the square and circular air coils. Section 4 discusses thermal modeling. Section 5 gives a detailed comparison of the two air coils. The final section summarizes the paper and provides concluding insights.

2. Operating principle

Air coils use the earth's magnetic field ($\vec{B}$), which changes with the altitude and inclination angle of the satellite. At a specific altitude and inclination angle the earth's magnetic field has different magnitude [8]. The dipole moment ($\vec{D}$) generated by the current carrying the air coil will interact with the earth's magnetic field and rotates the satellite in the specific direction [9] as described by the Fleming left hand rule in Figure 3.

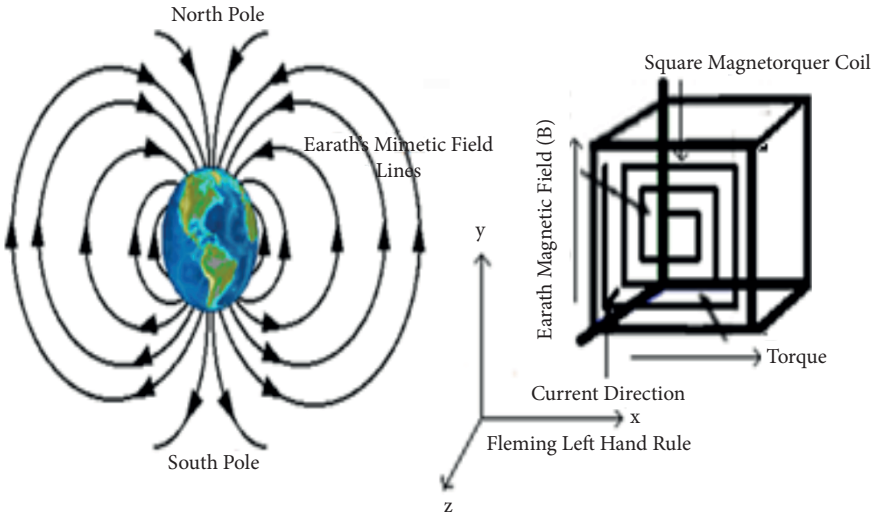

Figure 3. Earth's magnetic field interaction with air coil.

The generated magnetic moment ($\vec{D}$) is calculated by the following equation:

$$\vec{D} = N.S.I.\vec{n}, \tag{1}$$

where N = Number of turns in the coil,

S = Averaged surface area of the coil,

I = Current drawn by the coil

For the magnetic moment calculation, average surface area 'S' of the coil is taken. In Figure 4, the external side 'A' of the coil has a length of 79 mm and the corresponding internal side has a length of 29 mm. The average length is (79 + 29)/2 = 54 mm and the opposite side 'C' also has the same dimension. The two sides will have a total average length of 108 mm. Similarly, side 'B' has external length of 87 mm and the corresponding internal side has a length of 37 mm. The average length is (87 + 37)/2 = 62 mm and including side 'D', the two sides will have a total average length of 124 mm. The average length of the four sides of the

coil is 124 + 108 = 232 mm (as already shown in Table 1 with $L_{average}$ = 230 mm). As the coil has 50 turns, the total length is 230 × 50 = 11,500 mm as given in Table 1.

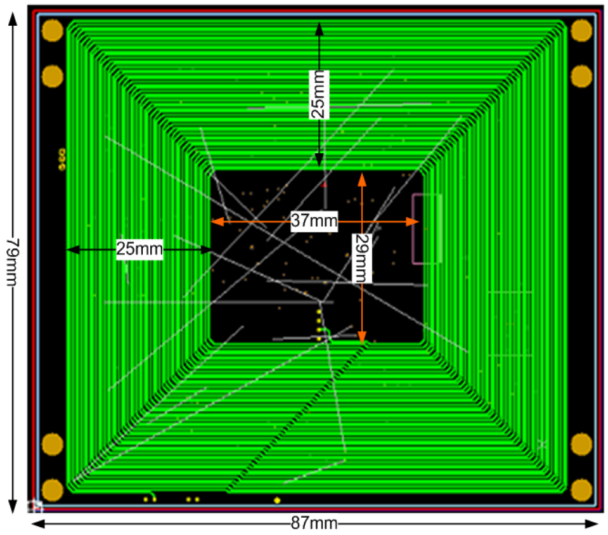

Figure 4. View and dimensions of a single square air coil [6,7].

Table 1. Dimensions parameters of square air coils.

Parameters	Values
Single turn average length; l avg	230 mm
Total length of single coil; Lt	11.5 m
Trace cross-sectional area; A = w × t	0.3 mm × 18 μm
Distance between two adjacent traces	0.2 mm
Bundle width (50 traces)	25 mm
Copper resistivity; ρ	1.68 × $10^8\Omega$m
Single coil resistance; R_o	36 ± 3Ω

Torque generated ($\vec{\tau}$) by the air coil can be calculated as follows:

$$\vec{\tau} = \vec{D} \times \vec{B} = \left|\vec{D}\right| \left|\vec{B}\right| \sin\theta \hat{n} \tag{2}$$

During the rotation of the satellite, for the generated torque calculations, a fixed angle (i.e. $\theta = 90^\circ$) is taken between the magnetic moment and the magnetic field. The main goal of this generated torque is orientation and stabilization of the satellite in any direction.

3. Air coil design

Air coils are integrated within the PCB internal layers occupying no excess space on the spacecraft. Each layer has a separate coil that can be connected/disconnected through switches. Rearranging these switches, one can alter the configuration of these coils by connecting them in series, parallel, or any hybrid combination while using one, two, three, or four coils. This reconfigurable design provides the option for generating different amounts

of dipole moment and resultant torque to stabilize and rotate the satellite. They are also called embedded air coils because they are embedded in the solar panel unit PCB four internal layers. The solar panel PCB is an 8 layer PCB. The top layer has solar panels, while the bottom layer (layer 8) contains the air coil driver electronic components. Layers 2, 3, 4, and 5 will have the embedded air coils. Layers 6 and 7 will have analogue and digital ground planes, in order to secure the electronic components from the generated magnetic field by the air coils.

The cross-sectional view of the CubeSat PCB module shows air coil traces, given in Figure 5. These air coils are specifically designed for AraMis-C1.

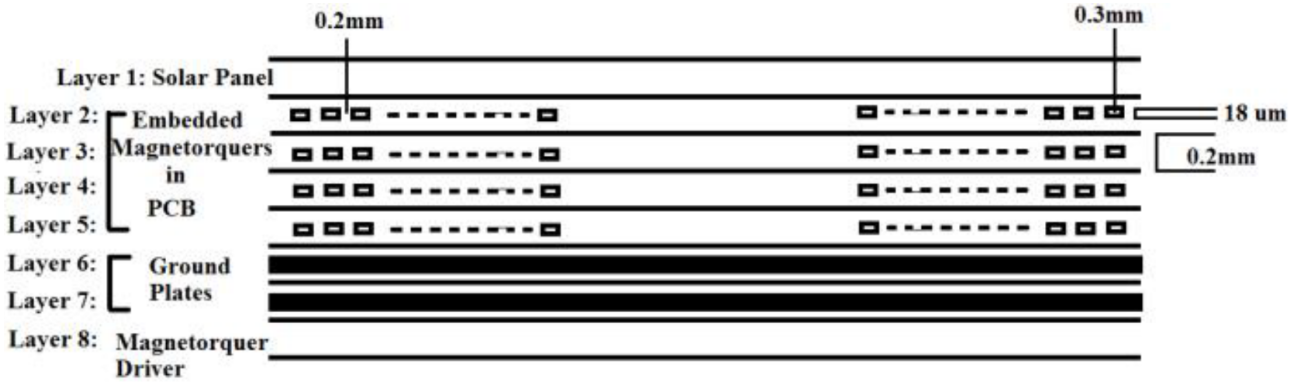

Figure 5. Cross sectional view of the CubeSat PCB module.

The coil in each layer has 50 turns and therefore the four internal layers of the CubeSat panel will have a total of 200 turns. The width of each coil trace is 0.3 mm and thickness is about 18 μm. The distance between two consecutive traces is 0.2 mm. Trace area (width $\times$ thickness), length, and number of turns of each coil affect the resistance of the air coil. The resistance allows specific current with respective applied voltage. The resultant current controls the dipole moment and results in power consumption and heat generated inside the CubeSat PCB.

Here is a brief description of two different shapes of air coil design, i.e. square and circular. The two coils have some common features, such as they have same trace width, thickness, and space between two adjacent traces. They are inserted inside the second, third, fourth, and fifth layers of the CubeSat module.

3.1. Square air coil

A view of the square coil along with dimensions in a single layer is shown in Figure 4. Table 1 highlights the key design parameters of the square air coil design. The main focus of the air coil design is to make it compatible with the CubeSat PCB dimensions by not only being lighter but also being able to generate the intended dipole moment [10]. With the dimensions' parameters given in Table 1, the designed square air coil has 36 Ω resistance. The amount of dipole moment generated is controlled by the amount of current.

3.2. Circular air coil

A view of the circular coil along with dimensions in a single layer is shown in Figure 6. Table 2 highlights the key design parameters of the circular air coil design. The CubeSat PCB's dimensions are 82.5 $\times$ 98 mm^2. The circular coil is embedded in the internal layers with radius of 39.5 mm. Fifty traces bundle occupies a space of 25 mm with each trace width 0.3 mm and 0.2 mm internal space between two adjacent traces as shown in

Figure 6. With the dimensions' parameters given in Table 2, the designed circular air coil has 26 Ω resistance. The amount of dipole moment generated is controlled by the amount of current [11].

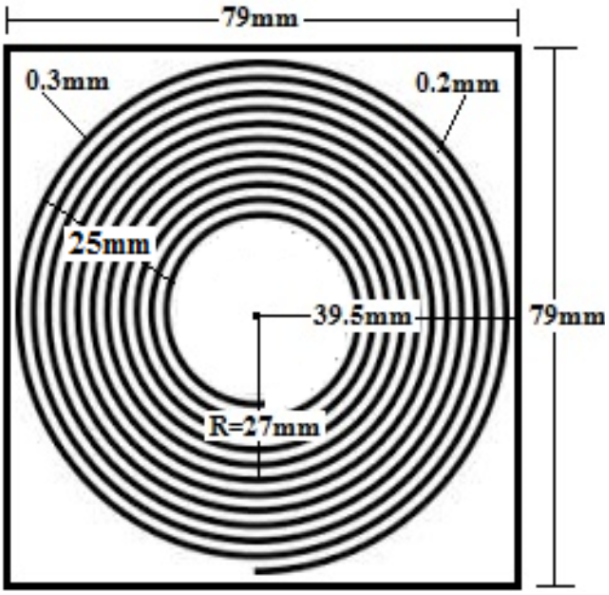

Figure 6. View and dimensions of a single circular air coil.

Table 2. Dimensions parameters of circular air coils.

Parameters	Values
Single turn average length; l avg	169.56 mm
Total length of single coil; Lt	8.478 m
Trace cross-sectional area; A = w × t	0.3 mm × 18 μm
Distance between two adjacent traces	0.2 mm
Bundle width (50 traces)	25 mm
Copper resistivity; ρ	$1.68 \times 10^8\,\Omega$m
Single coil resistance; R_o	$26 \pm 3\Omega$

Power consumption and time of rotation Power dissipated by the air coil can be calculated by

$$P = I^2 R, \tag{3}$$

where P is the power dissipated by the coil,

I is the current drawn by the coil,

R is the resistance of the coil.

The angular speed (ω) of a satellite depends on the torque exerted and moment of inertia (J) of the satellite. Suppose the satellite has to be rotated by an angle (Θ). When a constant torque ($\tau_{\max}$) is applied for a certain time ($T/2$), the angular speed (ω) increases linearly, while to stop the satellite an opposite torque of the same magnitude ($-\tau_{\max}$) and duration ($T/2$) is applied. The opposite torque seizes the satellite spin after covering exactly the desired angle (Θ) [8].

The generated torque is given by Newton's second law of rotation:

$$\tau = J\dot{\omega} \tag{4}$$

The angular position (Θ) is given by the following expression:

$$\theta = \dot{\omega}\left(\frac{T}{2}\right)^2 + \dot{\omega}\left(\frac{T}{2}\right)^2 = \frac{1}{2}\frac{\tau}{J}T^2 \tag{5}$$

The time T required for the air coil to rotate the satellite through a certain angle Θ is given by

$$T = \sqrt{\frac{2J\theta}{\tau}} \tag{6}$$

where T is the time required for rotation through an angle of θ° and J is the moment of inertia of AraMiS-C1, which is 0.0059 kgm^2.

4. Thermal modeling

Thermal modeling is the most important step in the design of an embedded air coil. When the air coil is energized, heat is produced as a result of power dissipation, which in turn increases the overall temperature of the PCB. This increase in temperature should not be greater than the CubePMT module design temperature limits [7]. Thermal modeling gives a detailed analysis of the power dissipation versus temperature variation of the CubePMT PCB. The amount of current drawn across the coil greatly changes the power dissipation and dipole moments. Thus, the PCB temperature increases with the increase in dipole moment [6]. The CubePMT module radiates and absorbs heat to and from the surroundings. Heat energy absorbed by the PCB from the surroundings is added to the heat generated by the air coils. This additional energy increases the overall temperature of the PCB [2].

In thermal equilibrium condition the total radiated heat power from the CubePMT module to the surroundings (P_o) is equal to the electrical power dissipated by the air coil inside the PCB (P_d) and power absorbed from the surroundings (P_I) depicted in Figure 7 and given in (7).

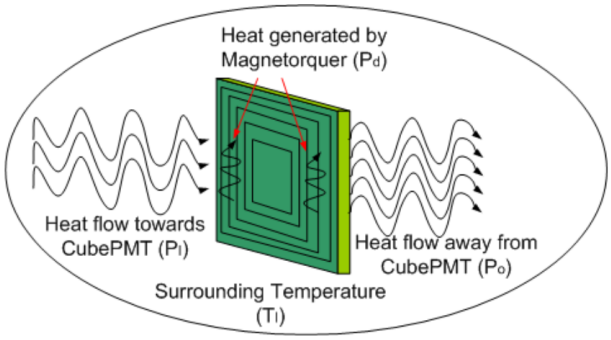

Figure 7. Heat flow through CubePMT module.

$$P_0 = P_d + P_I \tag{7}$$

The power dissipated by air coils (P_d) is given by (3) and the power radiated (P_o) from the PCB surface and power absorbed from the surrounding can be deduced from the Stefan–Boltzmann law [9]:

$$P_0 = \alpha_o \sigma T_o^4 S$$
$$P_I = \alpha_1 \sigma T_I^4 S \tag{8}$$

where 'α_I' and 'α_o' are the absorption coefficient and emissivity of the PCB surface, respectively. These parameters were measured in a laboratory experiment and were found equal with a value equal to 0.9. In the proceeding discussions the same symbol 'α' will be used for both emissivity and absorption coefficient.

Rearranging (5) and (6) will give the PCB surface temperature T_1 as given in (9):

$$T_o = \sqrt[4]{\frac{Pd + \alpha\sigma {T_1}^4 S}{\alpha\sigma S}} \tag{9}$$

where T_o is the PCB surface temperature in Kelvin,

α is the emissivity of the PCB material,

σ is the Stefan–Boltzmann constant = 5.6 $\times$ 10^{-8} W.m^{-2}.K^{-4},

T_1 is the surrounding temperature = 298.14 K,

S is the PCB surface area (both sides) = 0.016 m^2

In (7), all the parameters are known except emissivity (α), which was found through a laboratory experiment for the CubePMT module of AraMiS-C1.

5. Comparison

Square and circular embedded air coils are compared on the basis of dipole moment and torque generated, power consumption, temperature rise, and the resultant time required for the satellite rotation. The input voltage is varied from 0 V to 18 V and all the resultant parameters are measured. On the basis of these comparisons it was decided which shape of air coil is better. In the proceeding sections the comparison results of all the parameters of interest for square and circular air coils are plotted and discussed.

5.1. Applied voltage versus dipole moment generated

Dipole moment for different arrangements (single coil, four in series, 2 $\times$ 2 hybrid, and four in parallel) of square and circular air coils is measured against a span of applied voltage (0 V $\sim$ 18 V) and plotted in Figures 8a and 8b, respectively. The dipole moment of different combinations at 16 V is analyzed. Dipole moment generated by a single coil and four coils in series for square and circular air coils is the same and equal to 0.07 Am^2. Four coils in parallel of square air coils have a dipole moment 1.2 Am^2 and for circular air coils it is 1.13 Am^2. Hybrid combinations of square and circular air coils have a dipole moment of 0.3 Am^2 and 0.28 Am^2, respectively. These results demonstrate that square air coils offer better dipole moment than circular air coils.

5.2. Applied voltage versus power dissipated

In this subsection, power dissipated is compared with the applied voltage (0 V–18 V). At applied voltage of 16 V for square and circular air coils the power dissipated of all the possible combinations is measured as shown in Figures 9a and 9b, respectively. Power dissipated by single coil square air coils is 7.1 W and circular air coils is 9.8 W. Power dissipated by four coils in series, four coils in parallel, and hybrid combination of square air coils is 28.4 W and circular air coils is 39.4 W. The square air coils dissipate less power as compared to circular air coils in all four cases as shown in comparison.

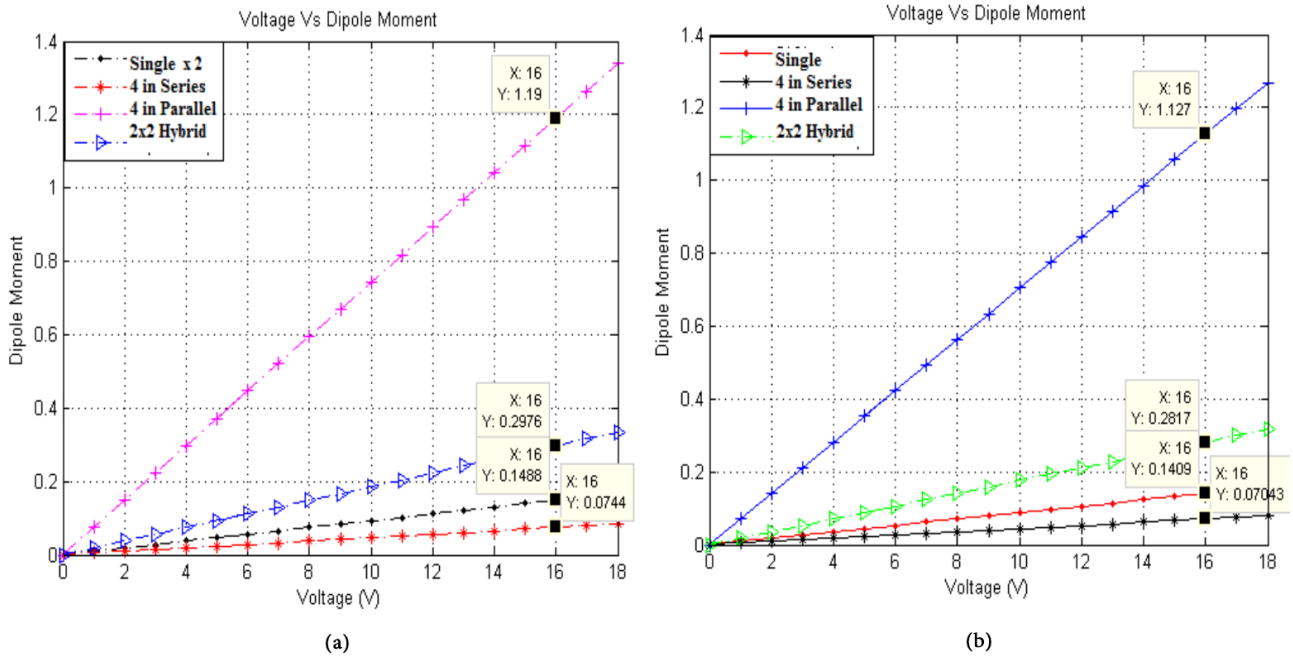

Figure 8. Voltage versus dipole moment of (a) square and (b) circular air coils.

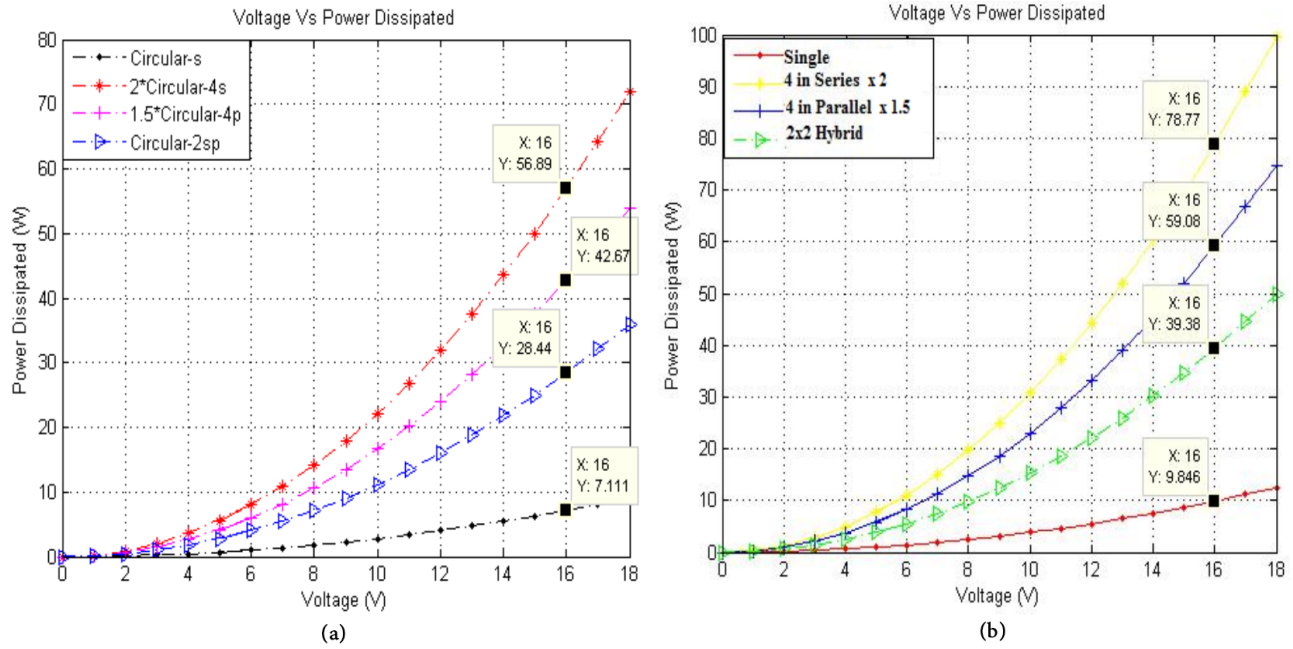

Figure 9. Voltage versus power dissipated of (a) square (b) circular air coils.

5.3. Applied voltage versus torque generated

The plot of voltage versus power and torque generated is compared for square and circular air coils as shown in Figures 10a and 10b, respectively, for all combinations. Torque generated by a single coil and four coils in series of the square air coil is 3.72 μNm and the circular air coil is 3.52 μNm. Torque generated by four coils in parallel configuration of the square air coil is 14.88 μNm and circular air coil is 14.09 μNm. Torque generated

by hybrid combination of square air coils is 7.44 μNm and circular air coils is 7.04 μNm. This comparison shows that square air coils generate better torque than circular air coils in all four cases.

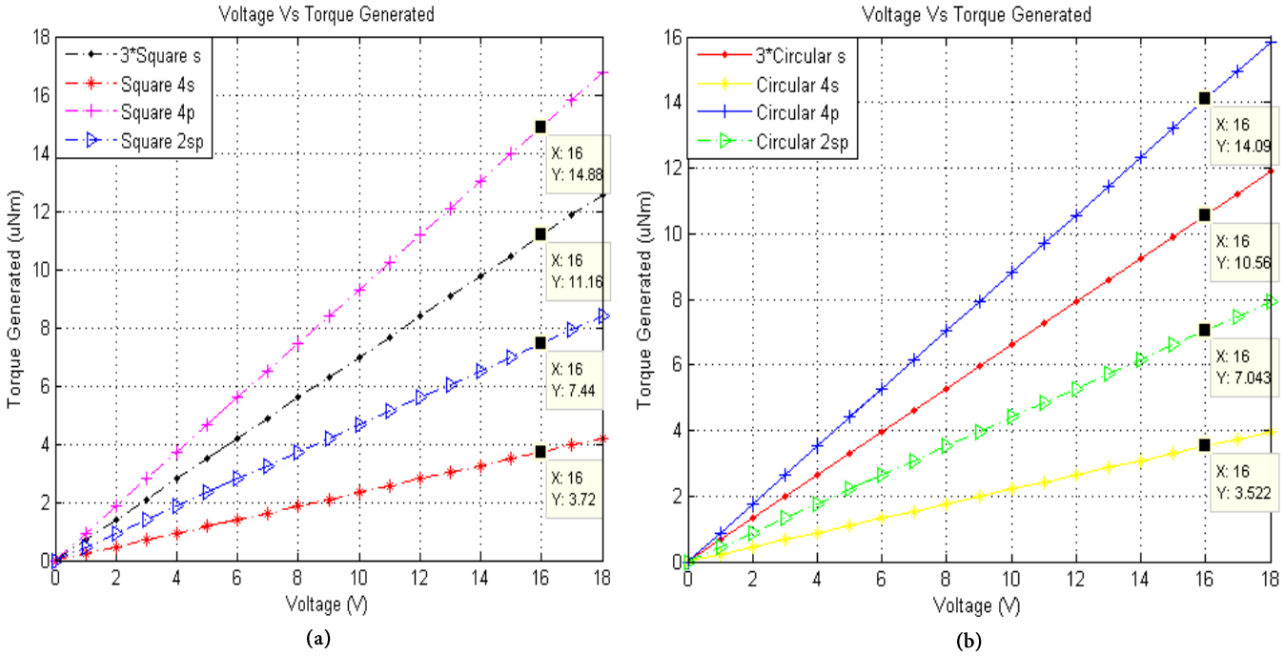

Figure 10. Voltage versus generated torque of (a) square (b) circular air coils.

5.4. Applied voltage versus temperature

The plots of voltage versus temperature and torque versus power dissipated are shown in Figures 11a and 11b, respectively. Temperature rise by single coil square air coils is 85.5 K and circular air coils is 102.3 K. Temperature rise by four coils in series, four coils in parallel, and hybrid combination of square air coils is 180.7 K and circular air coils is 212.65 K. The square air coils have smaller temperature rise than circular air coils in all four cases as shown in comparison.

5.5. Torque generated versus power dissipated

This subsection shows a comparison of torque generated versus power dissipated. At a power dissipation of 8 W in square air coils, the torque generated by a single coil is 4.19 μNm, the torque generated by four coils in series is 2.09 μNm, the torque generated by four coils in parallel is 8.37 μNm, and the torque generated by hybrid combination is 4.19 μNm. While at a power dissipation of 12.46 W in circular air coils the torque generated by single coil is 3.96 μNm, the torque generated by four coils in series is 1.981 μNm, the torque generated by four coils in parallel is 8.92 μNm, and the torque generated by hybrid combination is 3.96 μNm. The comparison shows that square air coils dissipate less power with a greater amount of torque generated while the circular air coils dissipates greater power with less torque generated. The plot of torque generated versus power dissipated is shown in Figure 12a of square and Figure 12b of circular embedded air coils, respectively.

5.6. Dipole moment versus torque generated

A single coil and four coils in series of square air coils generate the same dipole moment of 0.084 Am^2, which results in a torque of 4.18 μNm. Circular air coils provide 3.96 μNm torque as a result of 0.097 Am^2 dipole

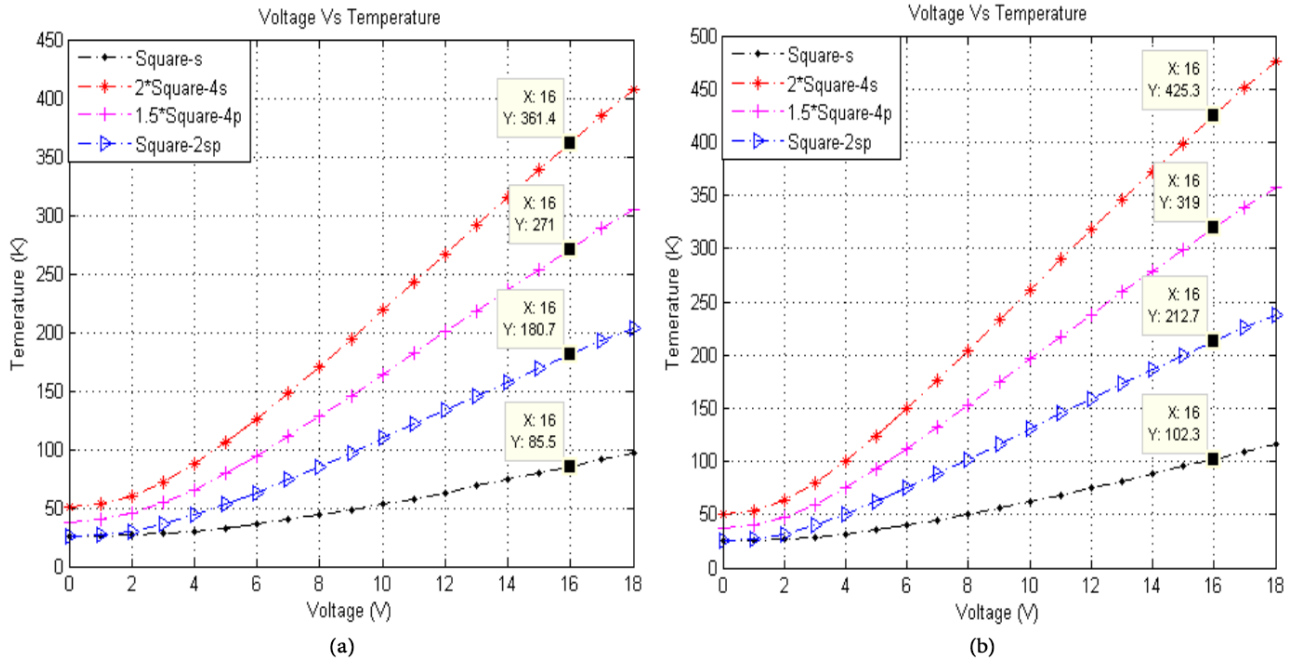

Figure 11. Voltage versus temperature of (a) square (b) circular air coils.

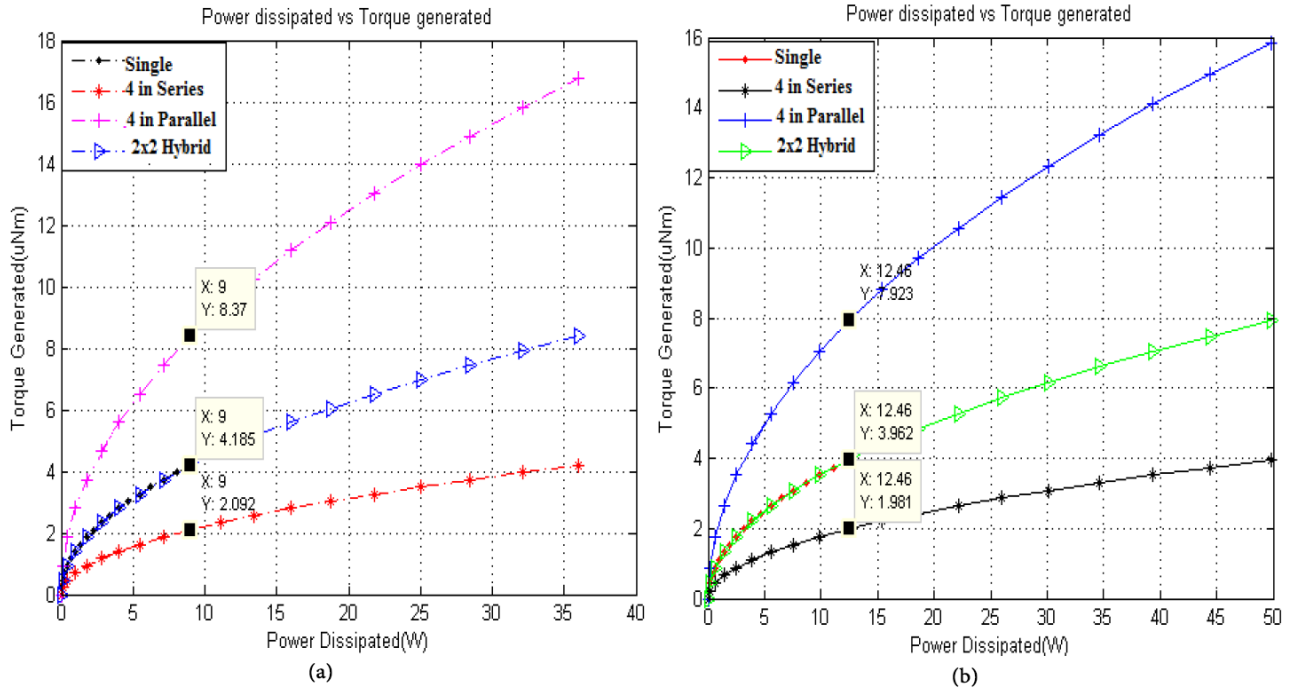

Figure 12. Torque generated versus power dissipated of (a) square (b) circular air coils.

moment. Four coils in parallel of square air coils generate 5.58 μNm torque, which has a dipole moment of 0.45 Am^2. Circular air coils generate dipole moment of 0.35 Am^2, which provides a torque of 4.40 μNm. Hybrid combination of square air coils generate 8.37 μNm torque, which has a dipole moment of 0.34 Am^2

and circular air coils have 7.92 μNm torque with 0.32 Am^2 dipole moment. The plot of dipole moment versus torque generated is shown in Figure 13a and Figure 13b for square and circular embedded air coils, respectively.

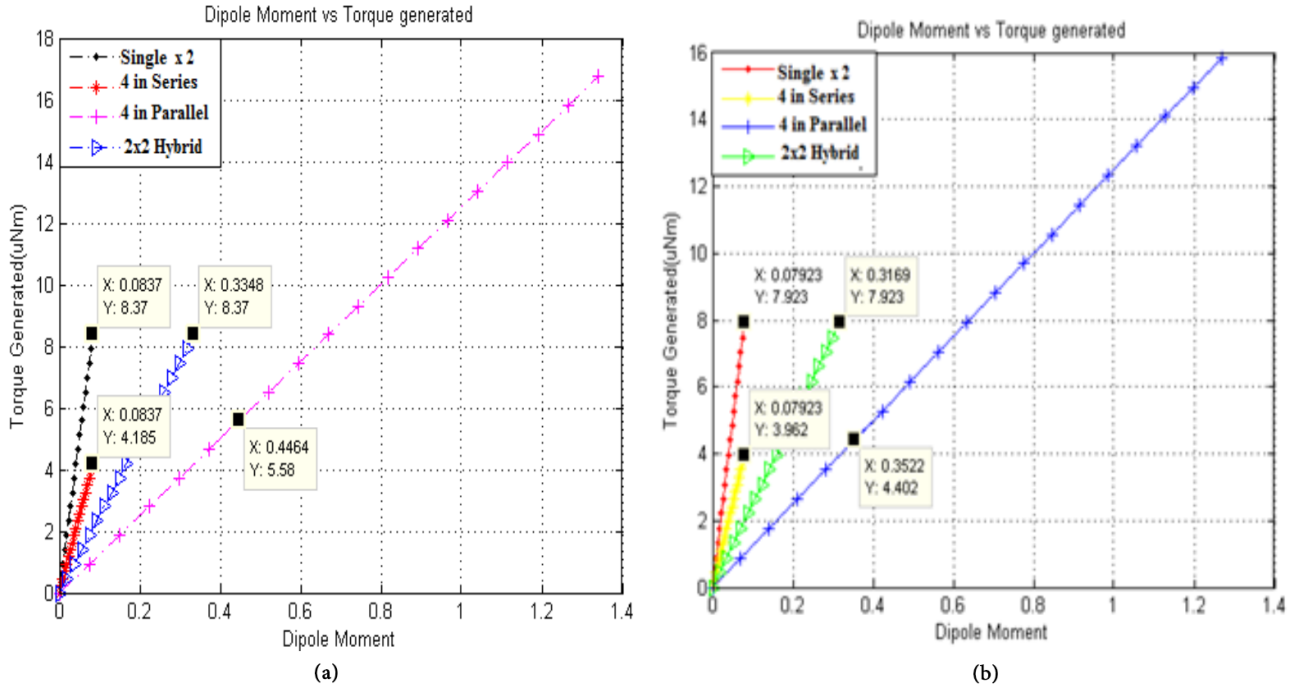

Figure 13. Dipole moment versus torque generated of (a) square (b) circular air coils.

5.7. Time of rotation versus generated torque

The discussion in this section focuses on the time taken by rotating AraMiS-C1 through 90° using different combinations of square and circular air coils. Square air coils of single coil require 46.98 s and 2 × 2 hybrid combination requires 66.64 s and both of them generates 8.37 μNm torque to rotate the satellite through an angle of 90°. In the case of circular air coils, a single coil requires 48.3 s and 2 × 2 hybrid combination requires 68.28 s and both of them generate 7.92 μNm torque to rotate the satellite at an angle of 90°. Four coils in series of square air coils generate 10.46 μNm torque, which takes 37.6 s, and that of circular air coils is 9.9 μNm, which takes 38.6 s to rotate the satellite through an angle of 90°. Four coils in parallel of square air coils generate 25.1 μNm torque, which takes 31.3 s, and circular air coil generates 23.8 μNm torque, which takes 32.2 s to rotate the satellite through an angle of 90°. In both cases, square and circular air coils, the graphs of a single coil is multiplied by 2, the four coils in series is multiplied by 2.5, and the four coils in parallel is multiplied by 1.5 to distinguish them from one another. The plots of time required versus torque generated are shown in Figure 14a for square and Figure 14b of circular embedded air coils, respectively.

6. Conclusion

In this paper, the design of two different shapes embedded air coils was discussed and their comparison was performed on the basis of dipole moment, torque generated, power dissipated, thermal modeling, and time of rotation. Air coils are embedded in four internal layers of an 8 layer PCB of CubePMT module. Embedded air coils are the best choice for the CubeSat attitude control system as compared to reaction wheels, permanent

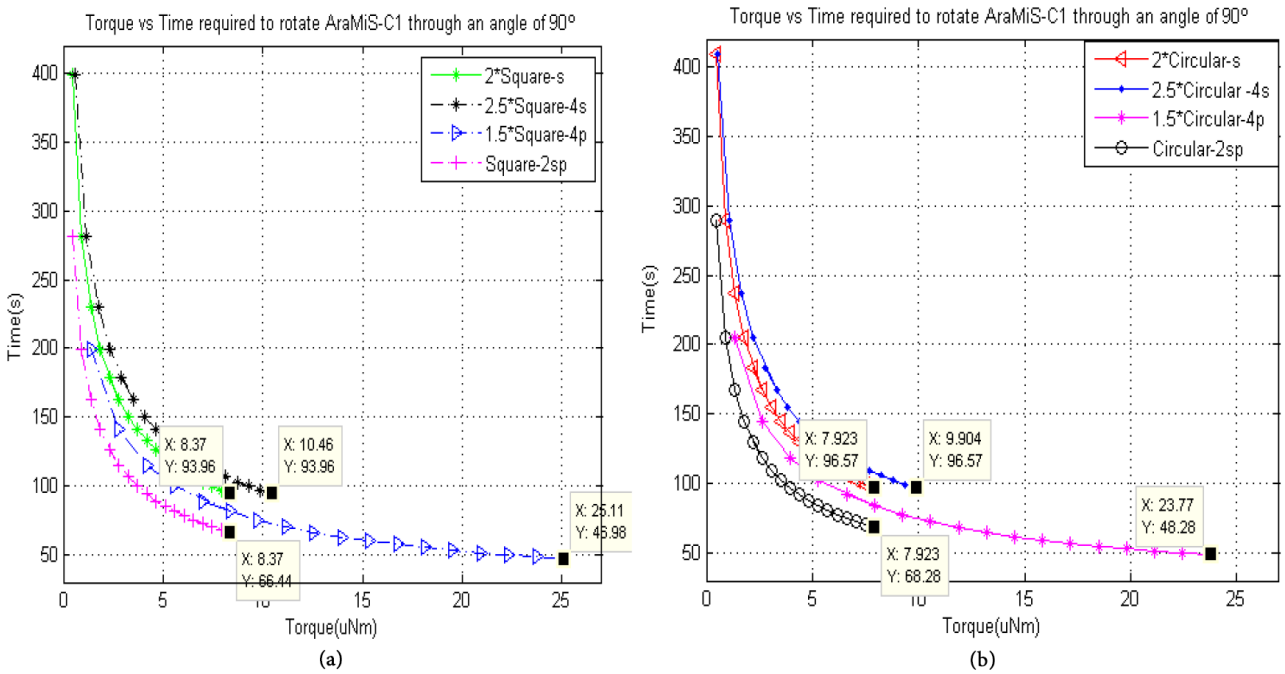

Figure 14. Torque generated versus time required for (a) square (b) circular air coils.

magnets, magnetic rods, and thrusters in terms of space occupation and weight. These coils are used for the rotation and stabilization of small satellites with miniaturized dimensions, low mass, and minimum heat dissipation.

The comparison between square and circular air coils illustrates that square air coils dissipate less power, produce more torque and dipole moment, require less time of rotation, and result in low temperature rise of the CubePMT module. Circular air coils dissipate more power, produce less torque and dipole moment, require more time of rotation, and result in high temperature rise. Thus, the square embedded air coil is the right option for the orientation control of the CubeSat Standard Nanosatellites in all aspects. Therefore, the square embedded air coil is used as attitude actuator for AraMiS-C1 attitude stabilization.

References

[1] Puig-Suari J, Turner C, Ahlgren W. Development of the standard CubeSat deployer and a CubeSat class PicoSatellite. 2001 IEEE Aerospace Conference Proceedings (Cat. No.01TH8542), Big Sky, MT, 2001, pp. 1/347-1/353 vol. 1.

[2] Alminde L, Bisgaard M, Vinther D, Viscor T, Ostergard K. Educational value and lessons learned from the AAU-CubeSat project. Proceedings of International Conference on Recent Advances in Space Technologies, 2003. RAST '03, Istanbul, Turkey, 2003, pp. 57-62.

[3] Hu Y, Wang D, Liu C. Reconfigurability research of satellite attitude control system under reliability constraints. Proceedings of the 33rd Chinese Control Conference, Nanjing, 2014, pp. 3244-3248.

[4] Shams N, Tanveer F, Ahmad S. Design and development of attitude control system (ACS) using COTS based components for small satellites. 2008 2nd International Conference on Advances in Space Technologies, Islamabad, 2008, pp. 6-11.

[5] Russell B, Clement L, Hernandez J, Byagowi A, Schor D, Kinsner W. Implementation of a nanosatellite attitude determination and control system for the T-Sat1 mission. 2013 26th IEEE Canadian Conference on Electrical and Computer Engineering (CCECE), Regina, SK, 2013, pp. 1-5.

[6] Mukhtar Z, Ali A, Mughal R, Reyneri L. Design and comparison of different shapes embedded magnetorquer coils for CubeSat standard nanosatellites. 2016 International Conference on Computing, Electronic and Electrical Engineering (ICE Cube), Quetta, Pakistan, 2016, pp. 175-180.

[7] Ali A, Mughal R, Ali H, Reyneri L, Aman N. Design, implementation, and thermal modeling of embedded reconfigurable magnetorquer system for nanosatellites. IEEE T Aero Elec Sys 2015; 51: 2669-2679.

[8] Rehman S, Marchand R, Berthelier J, Onishi T, Burchill J. Earth magnetic field effects on particle sensors on LEO satellites. IEEE T Plasma Sci 2013; 41: 3402-3409.

[9] Bakshi UA, Bakshi MV. Electromechanical Energy Conversion & D.C. Machines. First edition. Pune, India: Technical Publications, 2009.

[10] Howell JR, Mengüç MP, Siegel R. Thermal Radiation Heat Transfer, 6th edition. Boca Raton, FL, USA: CRC Press, 2015.

[11] Chen Z. Integrated electrical and thermal modeling, analysis and design for IPEM. PhD, Virginia Polytechnic Institute and State University, Blacksburg, VA, USA, 2004.